

PAPER

View Article Online  
View Journal | View Issue



Cite this: *Polym. Chem.*, 2022, **13**, 3705

# Interpenetrated triple network polymers: synergies of three different dynamic bonds†

Shiwanka V. Wanasinghe, Nethmi De Alwis Watuthanthrige and Dominik Konkolewicz \*

An ongoing challenge in soft materials is to develop networks with high mechanical robustness while showing complete self-healing and stress relaxation. In this study we develop triple network (TN) materials with three different polymers with distinct dynamic linkers (Diels–Alder, boronic acid-ester and hydrogen bonding). TN materials exhibit significant improvement of strength, stability and excellent self-healing properties simultaneously compared to their analogous double networks (DNs). All the TNs (TN-FMA 5%, 7% and 9%) show higher tensile strength over all DNs. In addition, TN-FMA (9%) demonstrates an excellent fracture energy over 20 000 J m<sup>−2</sup>, 750% elongation and fast stress relaxation. This highlights how dynamic bonding multiplicity and network structure can play a major role in improving the quality of dynamic materials.

Received 2nd May 2022,  
Accepted 26th May 2022

DOI: 10.1039/d2py00575a

rsc.li/polymers

## Introduction

Tuning the network structure of interpenetrating networks (IPNs) has drawn tremendous attention from the scientific community due to the resulting property enhancement.<sup>1</sup> These advanced structures lead to polymer materials with superior fracture energy, toughness, elasticity, and mechanical strength, making them promising candidates for various applications such as tires, seals, gloves, and other medicinal applications.<sup>2–5</sup> IPNs consist of multiple networks that are not covalently crosslinked with each other but woven into a ‘mesh’ like structure by sterics and entanglements.<sup>2,6,7</sup> Interchain entanglement forces or cohesive forces lock the structure of IPNs resulting in improved network percolation compared to that of Single Networks (SNs).<sup>8,9</sup> In contrast to IPNs, SNs comprise one type of network covalently bonded between all possible parts of the material.<sup>10</sup> However, the reduced energy dissipation mechanisms of SNs resulted in poor toughness in materials and limited their functions in practical applications.<sup>11–13</sup> Double Networks (DNs), a subcategory of IPNs, were introduced in 2003 and significant research has been conducted to understand the origins of the superior properties of DNs.<sup>1,11,14,15</sup> DNs consist of two networks interpenetrated with each other, typically with highly disparate structures and crosslink densities, resulting in hydrogels or elastomers with excellent mechanical properties compared to their

individual components.<sup>4,16</sup> However, most of these DN materials are static, with energy dissipation arising from irreversible cleavage of covalent bonds.<sup>17</sup>

Recently, the DN concept has been extended to Triple Networks (TNs) to optimize the material properties beyond those of the existing DN materials.<sup>5,12,18–22</sup> Most triple networks are formed by the addition of a third component into a DN, necessitating three network forming reactions.<sup>2,3</sup> Significant effort has been devoted to investigating the improvement of the properties of TNs.<sup>3,5,11,21</sup> Yet, the majority of TNs developed to date are non-dynamic linkers.<sup>3,5,23</sup> The incorporation of dynamic or reversible bonds into TNs is an interesting way of developing materials with better tunability and adaptiveness through a modular approach. Many studies have shown that SN materials have enhanced mechanical properties by the introduction of dynamic covalent and dynamic non-covalent bonds individually or as a combination of SNs and DNs.<sup>24–29</sup> A combination of different crosslinks in one material offers complementary properties such as improved strength, fast shape recovery and toughness.<sup>27,30–32</sup> However, it is still a challenge to simultaneously obtain high mechanical properties and fast (within 1 day), complete self-healing recovery under ambient conditions.

Previous studies have reported triply dynamic networks and triple networks with enhanced mechanical properties.<sup>3,5,23,33</sup> Despite the excellent progress in materials synthesis and development, there are still opportunities to enhance the recovery healing times,<sup>33</sup> self-healing efficiency,<sup>5,23</sup> elasticity,<sup>3,5,23</sup> and fracture toughness<sup>3</sup> of triply dynamic materials. As a critical example, Zhang *et al.* designed an outstanding triply dynamic material with high mechanical strength.<sup>33</sup> They combined

Department of Chemistry and Biochemistry, Miami University, Oxford, OH, 45056, USA. E-mail: d.konkolewicz@miamioh.edu

† Electronic supplementary information (ESI) available. See DOI: <https://doi.org/10.1039/d2py00575a>

metal-coordination, hydrogen-bonding and dynamic covalent urethane linkers into a single polymer chain, which ultimately resulted in triply dynamic SNs. These materials achieved 100% self-healing efficiency at room temperature, although this required 130 h (over 5 days).<sup>33</sup> Since most materials in day-to-day life have high heat resistance, it is desirable to obtain fast self-healing materials under heat rather than being slow at room temperature. In addition, Ducrot *et al.* synthesized TN polymer materials with excellent properties by introducing sacrificial bonds.<sup>3</sup> Although their materials showed excellent strength, their elongation and fracture toughness were relatively modest.<sup>3</sup> To the best of our knowledge, a modular approach to design complete dynamic TNs has not been explored yet. In the existing reports, either TNs have dynamic bonds only in parts of the networks, thus lacking the benefits of a hierarchical sequence of dynamic linkers, or the triple dynamic linkers are on a common backbone, thereby lacking the benefit of modular network synthesis and interpenetration (Scheme 1).

Diels–Alder chemistry, boronic ester chemistry and hydrogen-bonding (H-bonds) are three distinct dynamic chemistries that can be used in building multidynamic networks. UPy units are one of the most popular H-bond crosslinking motifs due to their simple synthesis, high association constant and versatility.<sup>34</sup> UPy units form both end-to-end dimers *via* a quadruple H-bond and stacks, thereby improving the mechanical strength, toughness and elongation due to the dissociation of UPy units upon stretching.<sup>34</sup> The pendant furan group in FMA can undergo a Diels–Alder reaction with an electron-poor alkene. The Diels–Alder adducts are thermoresponsive motifs which are static under ambient conditions and dynamic upon heating *via* the retro-Diels–Alder reaction. This static nature of Diels–Alder adducts provides stable materials at room temperature exhibiting high creep resistance.<sup>35,36</sup> In contrast to these two linkers, the reversibility of boronic esters and boronates can be activated even under humid conditions at room temperature thus providing adaptable self-healing and reprocessable materials in many environments.<sup>37,38</sup> Combination of these three distinct linkers with different timescales will provide adaptable materials with high mechanical robustness. Furthermore, the incorporation of each linker into its own polymer chain enables a modular approach to materials

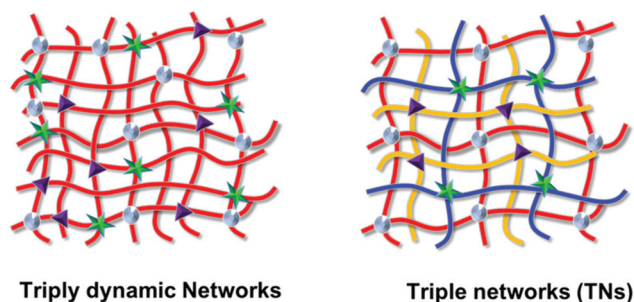
design, as well as facilitates effects such as entanglements and network dynamics, typical of IPNs. Nevertheless, these chemistries have been employed individually or as pairs to design SNs and IPNs including DNs and TNs to attain excellent mechanical properties.<sup>39–42</sup>

This study develops a novel triple network elastomer using a combination of dynamic covalent (Diels–Alder and boronate ester) and non-covalent (H-bonds) bonds to improve the mechanical robustness and dynamic characters of the materials. Polymers with pendant 2-ureido-4[1H]-pyrimidinone acrylate (UPyA), furfuryl methacrylate (FMA) and glyceryl acrylate (GA) were synthesized, combined, and finally crosslinked to acquire TNs with an orthogonal dynamic linker in each network (Scheme 2). Individual network components in the triple network elastomer were orthogonally crosslinked in one pot to yield the TN. Enhanced strength and fracture energies are expected, through the synergy between three unique linkers and the triple interpenetration, both of which are anticipated to lead to effective energy dissipation. Furthermore, introducing UPy and boronic ester bonds can accelerate the dynamic exchanges under ambient conditions and lead to efficient stress relaxation, in addition to the energy dissipation properties. Finally, the Diels–Alder units are introduced as static linkers at room temperature for strength and creep resistance, with full dynamic character upon heating leading to full self-healing in 24 h.

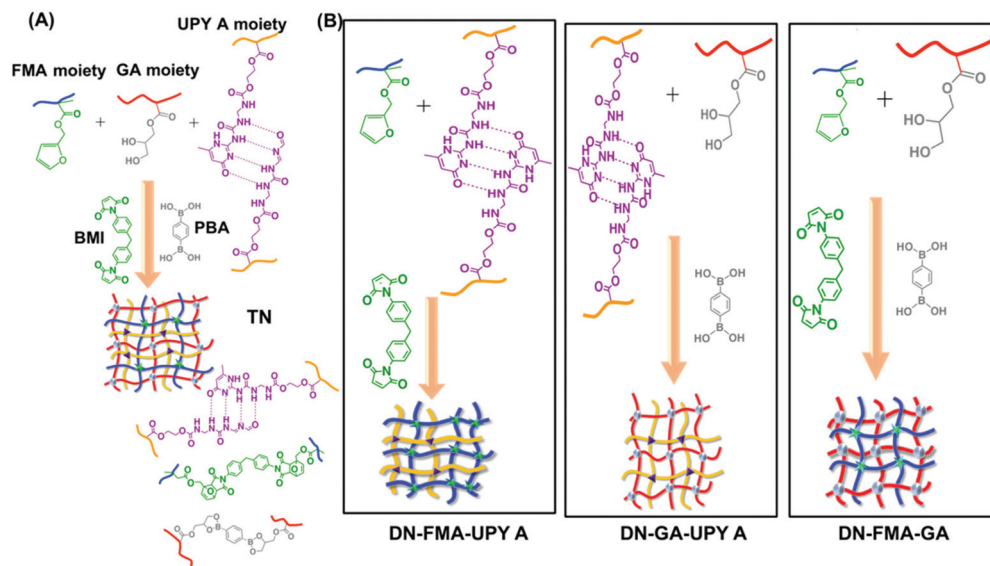
## Results and discussion

Ethyl acrylate was used as the backbone monomer for all three polymers synthesized using free radical polymerization. Each polymer was synthesized by introducing the crosslinker separately. Each polymer synthesized was soluble in the polar mixed solvent of methanol:*N,N*-dimethylformamide (DMF) in a 1:1 ratio. DNs and TNs were prepared by mixing particular polymers in a 1:1 ratio and a 1:1:1 ratio (by weight) respectively. Polymers with each crosslinker are denoted as poly-UPyA, poly-FMA and poly-GA. Three types of DN materials with UPyA, GA and FMA were prepared to compare the material properties with TNs: DN-FMA-UPyA, DN-FMA-GA and DN-GA-UPyA. A series of TNs were prepared by using different amounts of FMA (5%, 7%, and 9%) in the material and are named TN-FMA (5%), TN-FMA (7%) and TN-FMA (9%). The FMA crosslink density alone was varied in the TN materials since the essentially permanent crosslinks at room temperature, arising from FMA-based Diels–Alder linkages, can be used to modulate the materials strength and modulus. In contrast, efficient energy dissipation and transient hydrogen and boronic ester bond exchanges are anticipated while focusing on the essentially permanent linkers under ambient conditions.

The materials were subsequently dried and analyzed by infrared spectroscopy. As shown in Fig. S13,† negligible amounts of solvents remained, with no peak at 1500 cm<sup>−1</sup> in any sample, which is attributed to the C–N stretching of DMF.<sup>43</sup> The tensile test, fracture energy test and frequency sweep, self-healing, creep recovery and stress relaxation experi-



**Scheme 1** Schematic of triply dynamic networks and triple networks.



**Scheme 2** Schematic representation of the synthesis of networks. (A) Preparation of TNs. BMI (1-[4-[[4-(2,5-dioxopyrrol-1-yl)phenyl]methyl]phenyl]pyrrole-2,5-dione), PBA (phenyldiboric acid). (B) Preparation of DNs.

**Table 1** Properties of materials, stress at break, strain at break, fracture energy and glass transition temperature ( $T_g$ )

Entry	Network composition	Stress at break (kPa)	Strain at break (mm mm <sup>-1</sup> )	Fracture energy (J m <sup>-2</sup> )	$T_g$ (°C)
1	DN-FMA-UPyA	110 <sup>a</sup> ± 30	20 <sup>b</sup> ± 5	34 000 ± 3000	-12.2
2	DN-FMA-GA	25 <sup>a</sup> ± 4	20.5 <sup>b</sup> ± 0.7	7600 ± 500	-10.4
3	DN-GA-UPyA	290 ± 60	6.0 ± 0.7	3300 ± 600	-8.8
4	TN-FMA (5%)	370 ± 70	8 ± 1	6600 ± 100	-11.0
5	TN-FMA (7%)	510 ± 40	8.3 ± 0.9	10 000 ± 1000	-9.3
6	TN-FMA (9%)	350 ± 50	7 ± 4	21 000 ± 2000	-8.7

<sup>a</sup> Values are calculated as an average of the stress at break and maximum stress ( $n = 3$ ). <sup>b</sup> Values are calculated as an average of the strain at break and maximum strain.

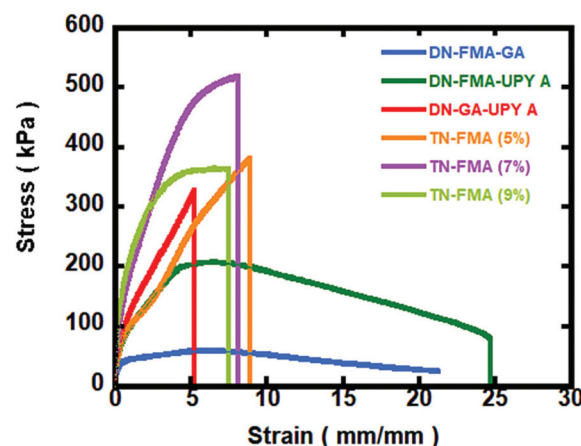


**Fig. 1** Stress-strain curves of all DNs and TNs.

ments were carried out to evaluate the properties of these materials.

All materials show similar  $T_g$  values, determined by DSC. These DSC data (Fig. S1†) reveal that both DNs and TNs have similar backbone mobility conferring similar thermal properties in all samples (Table 1). In the TN materials (Table 1, entries 4 to 6) there is a measurable increase in  $T_g$  moving from the 5% to the 7% FMA system, and a slight increase in  $T_g$  moving from the 7% to the 9% system. The increase in  $T_g$  with a higher crosslink density is expected, although the small change between 7% and 9% FMA could be due to clustering of Diels-Alder linkers, rather than well-percolated crosslinkers throughout the matrix. The typical stress-strain curves of all materials are given in Fig. 1. DN-FMA-UPyA and DN-FMA-GA networks displayed large strain at break (~2000%) compared to all the other materials (Table 1). Although they have higher elongation, all DNs exhibit low stress values compared to TNs. In particular, DN-FMA-GA has a very low peak stress value of

50 kPa. This is possibly due to the limited number of intertwining chains and fewer entanglements, combined with the rapid exchange of both boronate and UPy linkers in particular DN systems. In contrast, TN materials exhibit a greater number of entanglements, and hence stronger intermolecular locking forces, which could lead to a stronger material. Increasing the FMA amount from 5% to 7% raised the effective crosslinking points in the essentially permanent linkers, improving the tensile strength of the TN systems. However, further increasing the FMA percentage from 7% to 9% did not lead to substantial improvements in the tensile strength, with negative impacts on the strain at break. This could be due to the accumulation of Diels-Alder linkers as clusters within the network during the crosslinking process, which could weaken the overall network structure.

Fracture energy was measured by the paired “notched” and “pristine” approach described in the literature.<sup>44</sup> Notches were introduced into each “notched” specimen to half of the sample’s width. Each notched sample was extended to the break of the “notched” sample. The mean strain at which the notched samples fail, or fracture strain, is denoted as  $\epsilon_{\text{notch}}$ . The fracture energy ( $\Gamma$ ) is evaluated using the equation below:

$$\Gamma = h \int_0^{\epsilon_{\text{notch}}} \sigma d\epsilon \quad (1)$$

where  $h$  is the “pristine” sample’s initial height,  $\sigma$  is the “pristine” sample’s stress, and  $\epsilon$  is the “pristine” sample’s strain. The calculated fracture energies of all the materials are shown in Fig. 2. In general, TN systems demonstrated relatively higher fracture energies compared to DN systems except for DN-UPyA-FMA. DN-UPyA-FMA had the highest fracture energy ( $34\,000 \pm 3000 \text{ J m}^{-2}$ ) compared to all other materials. This excellent fracture energy is primarily due to the large fracture strain ( $\epsilon_{\text{notch}}$ ) observed in DN-FMA-UPyA and is consistent with its excellent tensile properties as shown in Fig. 1. Otherwise, its fracture stress is closer to that of TN-FMA (5%). The fracture energies of TN materials improved with the increment of FMA percentages in the networks resulting in the highest fracture energy for TN-FMA (9%) of  $21\,000 \pm 2000 \text{ J m}^{-2}$ . It is worth noting that these novel TN materials can be modulated through crosslink densities to obtain superior fracture energies and tensile strengths, without creating polymers that yield in tensile tests. In contrast, the DN-UPyA-FMA material had excellent fracture energy but relatively poor tensile strength and significant yielding characteristics.

Furthermore, the DNs and TNs were characterized through dynamic mechanical analysis experiments. Moduli of the materials were characterized by frequency sweep experiments as shown in Fig. 3. As predicted, TNs displayed higher storage and loss moduli compared to DNs in frequency sweep experiments, which was in accordance with our hypothesis. The superior internetwork entanglements and increment in

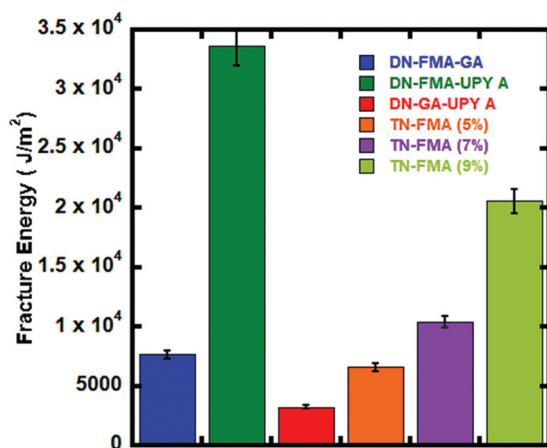


Fig. 2 Fracture energy of DNs and TNs. Fracture energy was calculated by testing “cut” and “uncut” materials and taking the average.

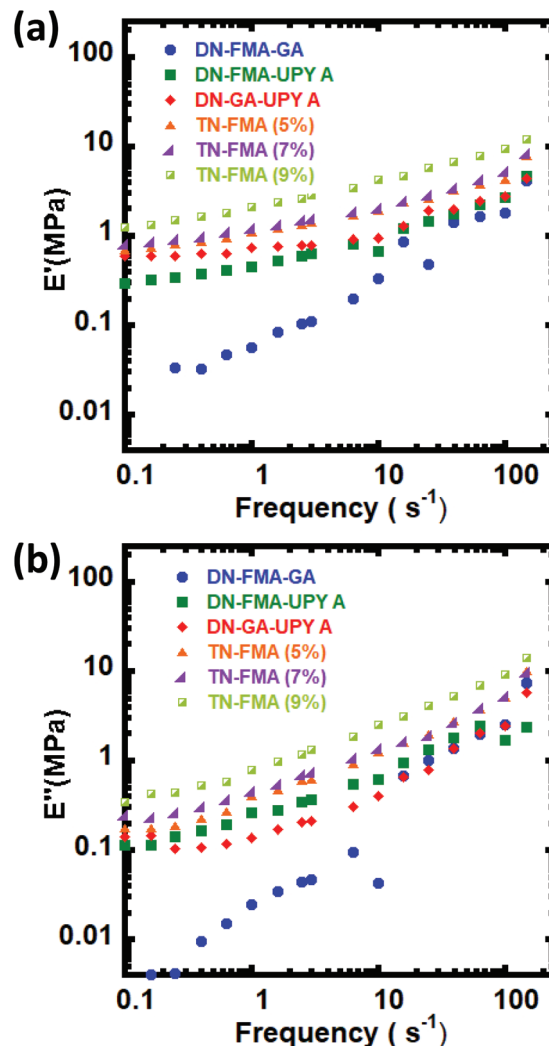


Fig. 3 Frequency sweep data of DNs and TNs. (a) Storage modulus ( $E'$ ) and (b) loss modulus ( $E''$ ) are shown.

effective crosslinking points contributed to improve the moduli in TN systems. This suggests that the ability to both store energy through a higher crosslink density and dissipate energy through exchange of dynamic bonds is improved in TNs compared to DNs. In addition, these frequency sweep data revealed that the storage modulus and loss modulus increase with the FMA percentage in the system, with the highest storage and loss moduli in TN-FMA (9%) and the lowest in TN-FMA (5%). This agrees with the common trend that the crosslinking density is proportional to the storage modulus.<sup>10</sup>

To investigate the bond exchange timescales, stress relaxation experiments were conducted by applying constant 20% strain. Fig. 4 illustrates the stress relaxation curves of the materials over 4 hours. The stress relaxation results revealed that all materials display essentially full relaxation within one hour under constant strain (Fig. 4). The stress relaxation data were fitted with a stretch exponential function, yielding relaxation times on the order of 100 s for each system. The relax-



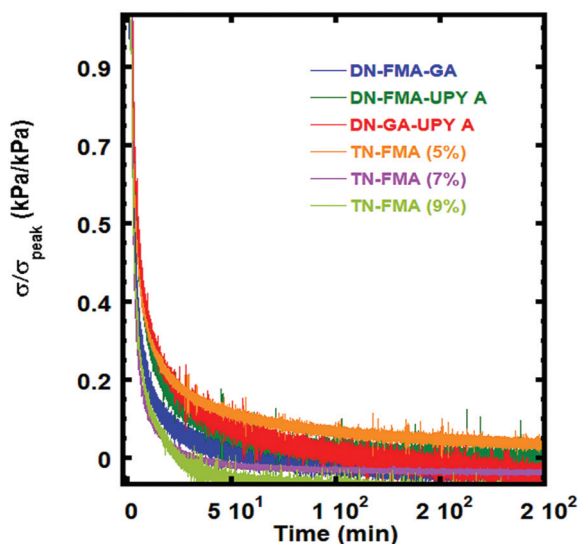


Fig. 4 Stress relaxation of materials. 15 point average of stress was calculated to plot the graph.

ation time and the exponent of the stretch exponential for each material are given in Table S1.† Faster stress relaxation was observed for TNs compared to DNs. However, TN-FMA (9%) showed slower relaxation compared to TN-FMA (7%). This is possibly due to the cluster formations of the TN-FMA (9%) sample which led to poor homogeneity of crosslinkers. The relaxation of each of these clusters can be different from the well dispersed linkers resulting unexpected slower relaxation compared to TN-FMA (7%). This excellent stress relaxation could arise from the faster exchange dynamics of UPyA and boronic ester dynamic systems at room temperature,<sup>34,37,38</sup> while DA bonds contribute minimally due to their essential stimuli responsive nature at elevated temperature.<sup>35,36</sup>

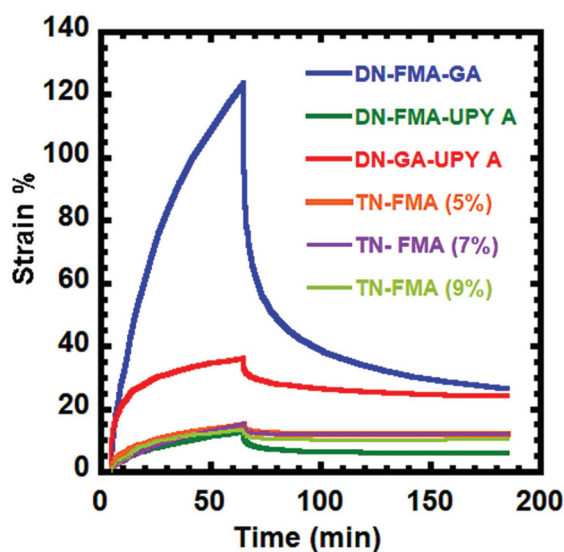


Fig. 5 Creep and creep recovery curves of all materials by applying 5 kPa stress for 1 h and 2 h for recovery.

The stability of the materials under near ambient conditions was investigated by conducting creep and creep recovery experiments (Fig. 5). The creep and creep recovery results indicated that all materials have high creep resistance except DN-FMA-GA and DN-GA-UPyA. In particular, the TNs had

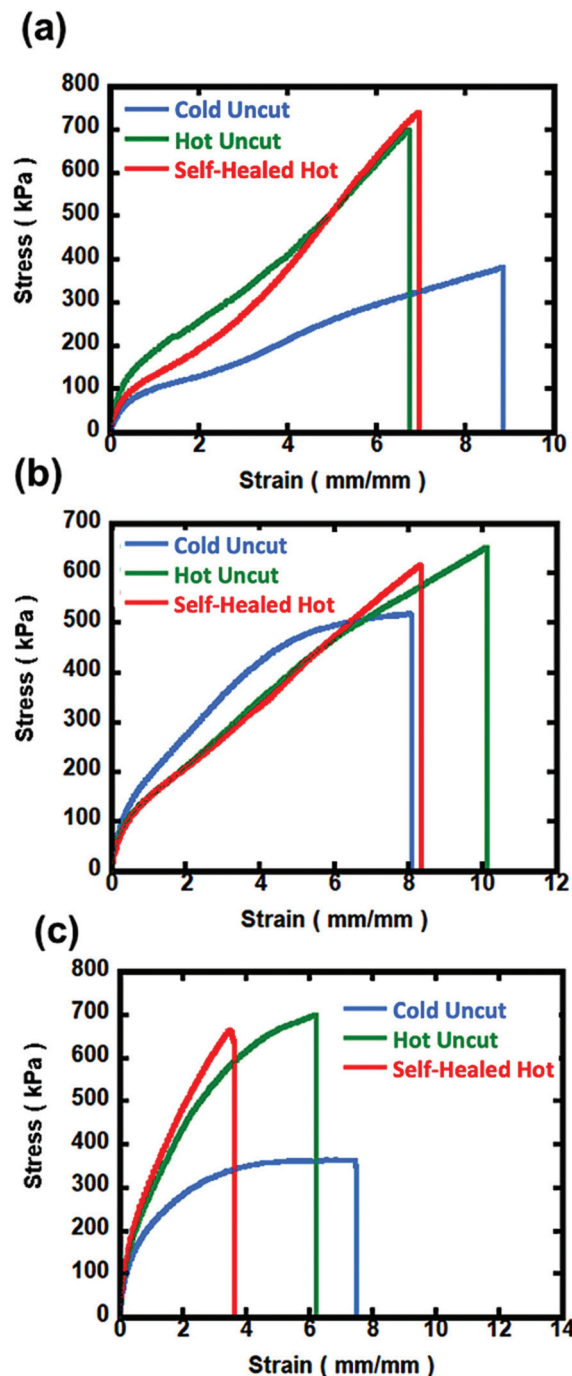


Fig. 6 Self-healing results of TN materials heated at 90 °C for 24 h. Unheated materials are denoted as "cold uncut". 24 h heated uncut materials are denoted as "hot uncut". (a) Self-healing curves of TN-FMA (5%). (b) Self-healing curves of TN-FMA (7%). (c) Self-healing curves of TN-FMA (9%).

vastly superior creep properties to DN-FMA-GA and DN-GA-UPyA. Surprisingly, all TNs (5%, 7%, and 9%) showed similar creep and creep recovery.

The dynamic properties of the TNs were further evaluated using self-healing experiments as shown in Fig. 6. In this test, materials were heated at 90 °C for 24 h. Heating improved the tensile stress of the materials, which could be due to the reduction of defects in the systems during heating.<sup>10</sup> All TNs showed essentially complete stress recovery within 24 h. This excellent self-healing and recovery of peak stress could be a consequence of the activation of exchange dynamics of all three reversible bonds in the systems with the addition of heat as an external stimulus. Both 5% and 7% materials displayed significantly greater self-healing profiles. However, TN-FMA (9%) samples showed ~60% recovery of the strain. The poorer healing in the TN-FMA (9%) materials could be due to the potential of crosslink-cluster formation in the network, which can inhibit effective exchange of all the DA linkers, limiting the full extensibility of the particular material. In this case, most of the crosslinks could recover, leading to good recovery in stress, yet cluster formation could prevent full percolation of the crosslinks, limiting elasticity. The DN-FMA-GA materials exhibited good self-healing efficiency than the DN-FMA-UPyA and DN-GA-UPyA materials. However, the tensile stress of self-healed DN materials is still lower than that of the TNs (Fig. S2–S4†).

A summary of the synthesized DN and TN materials in this work, as compared to other comparable materials in the literature,<sup>35,44–47</sup> is given in Fig. 7 in an Ashby plot. Foster *et al.* reported doubly dynamic materials crosslinked with UPyA (2.5%) and FMA (2.5%) linkers.<sup>35</sup> In 2020, Cummings *et al.* designed dynamic hydroxyethyl acrylate and ethyl acrylate materials using the UPyA crosslinker. In their study, they

demonstrated the effect of the matrices on the properties of the materials.<sup>44</sup> Cao *et al.* synthesized strong poly(ethylacrylate)-based elastomers hydrogen bonded with ionic liquids at room temperature.<sup>47</sup> In their work, the tunability of materials properties using the effect of the crosslinker concentration in the first network was studied. In 2020, Lei and coworkers reported a polyacrylamide (PAA) hydrogel cross-linked with eight tandem repeat proteins (G8).<sup>46</sup> They studied the effect of the crosslinker composition on the mechanical behaviors of the PAA-G8 hydrogel.<sup>46</sup> Sun *et al.* reported a stretchy tough hydrogel using acrylamide and alginate. They changed the weight ratios of acrylamide to acrylamide plus alginate to study the reason for the higher stretchability of the materials.<sup>45</sup> In general, the TN materials show better strength and fracture energy combined properties, suggesting that this is a viable strategy for new materials development.

## Conclusion

In summary, we designed and synthesized a novel TN material with enhanced mechanical properties including tensile strength, good stability, fast relaxation, and highest modulus while exhibiting better self-healing efficiency. These TNs contained three orthogonal dynamic bonds, dynamic hydrogen bonds through the UPy linker, dynamic boronate esters, and thermally responsive furan–maleimide Diels–Alder adducts. The TNs were all stronger than their double network counterparts, confirming that network multiplicity has strengthened the polymer network. In addition, all TNs have higher creep resistance than DN-FMA-GA and DN-GA-UPyA. The modular approach enables the synthesis of materials with distinct crosslink densities in each network. This leads to the targeted properties, such as TN-FMA (9%) having a high fracture energy of  $21\,000 \pm 2000 \text{ J m}^{-2}$  and the highest modulus. Additionally, due to the synergies of the crosslinks, all triple networks show ~100% self-healing stress recovery after heating at 90 °C for 24 h.

## Conflicts of interest

The authors declare no conflicts.

## Acknowledgements

This work was partially supported by the National Science Foundation under Grant No. (DMR-1749730) to D. K. The 400 MHz NMR instrumentation at Miami University is supported through funding from the National Science Foundation under grant number (CHE-1919850). D. K. acknowledges equipment support from Miami University through the Robert H. and Nancy J. Blayney Professorship.

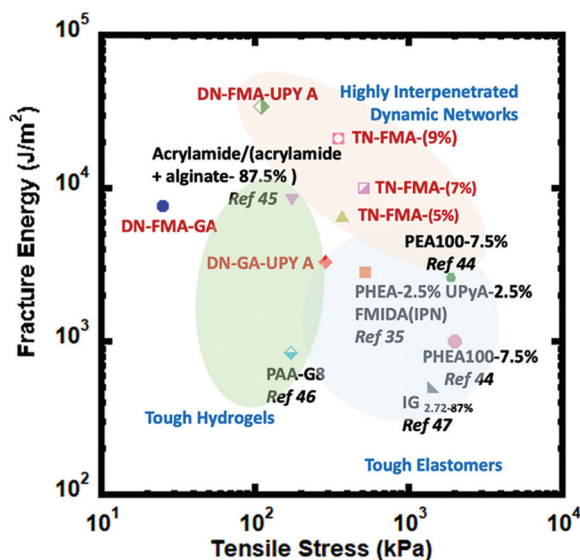


Fig. 7 Summary of tensile stress, fracture energy and creep resistance of all DNs and TNs (labeled in red) compared to several materials in the literature.<sup>35,44–47</sup>

## References

- Q. Chen, H. Chen, L. Zhu and J. Zheng, Fundamentals of Double Network Hydrogels, *J. Mater. Chem. B*, 2015, 3(18), 3654–3676.
- P. A. Panteli and C. S. Patrickios, Multiply Interpenetrating Polymer Networks: Preparation, Mechanical Properties, and Applications, *Gels*, 2019, 5(3), 36.
- E. Ducrot, Y. Chen, M. Bulters, R. P. Sijbesma and C. Creton, Toughening Elastomers with Sacrificial Bonds and Watching Them Break, *Science*, 2014, 344(6180), 186–189.
- T. Nakajima, H. Sato, Y. Zhao, S. Kawahara, T. Kurokawa, K. Sugahara and J. P. Gong, A Universal Molecular Stent Method to Toughen Any Hydrogels Based on Double Network Concept, *Adv. Funct. Mater.*, 2012, 22(21), 4426–4432.
- A. Argun, V. Can, U. Altun and O. Okay, Nonionic Double and Triple Network Hydrogels of High Mechanical Strength, *Macromolecules*, 2014, 47(18), 6430–6440.
- E. S. Dragan, Design and Applications of Interpenetrating Polymer Network Hydrogels. A Review, *Chem. Eng. J.*, 2014, 243, 572–590.
- L. H. Sperling, *Interpenetrating Polymer Networks and Related Materials*, Springer Science & Business Media, 2012.
- A. H. Landrock, *Handbook of Plastic Foams: Types, Properties, Manufacture and Applications*, Elsevier, 1995.
- S.-Q. Wang, Y. Wang, S. Cheng, X. Li, X. Zhu and H. Sun, New Experiments for Improved Theoretical Description of Nonlinear Rheology of Entangled Polymers, *Macromolecules*, 2013, 46(8), 3147–3159.
- S. V. Wanasinghe, E. M. Schreiber, A. M. Thompson, J. L. Sparks and D. Konkolewicz, Dynamic Covalent Chemistry for Architecture Changing Interpenetrated and Single Networks, *Polym. Chem.*, 2021, 12(13), 1975–1982.
- T. Sedláčik, T. Nonoyama, H. Guo, R. Kiyama, T. Nakajima, Y. Takeda, T. Kurokawa and J. P. Gong, Preparation of Tough Double-and Triple-Network Supermacroporous Hydrogels through Repeated Cryogelation, *Chem. Mater.*, 2020, 32(19), 8576–8586.
- Y. Wang, J. Niu, J. Hou, Z. Wang, J. Wu, G. Meng, Z. Liu and X. Guo, A Novel Design Strategy for Triple-Network Structure Hydrogels with High-Strength, Tough and Self-Healing Properties, *Polymer*, 2018, 135, 16–24.
- G. C. Ingavle, L. W. J. Baillie, Y. Zheng, E. K. Lis, I. N. Savina, C. A. Howell, S. V. Mikhailovsky and S. R. Sandeman, Affinity Binding of Antibodies to Supermacroporous Cryogel Adsorbents with Immobilized Protein A for Removal of Anthrax Toxin Protective Antigen, *Biomaterials*, 2015, 50, 140–153.
- M. A. Haque, T. Kurokawa and J. P. Gong, Super Tough Double Network Hydrogels and Their Application as Biomaterials, *Polymer*, 2012, 53(9), 1805–1822.
- J. P. Gong, Y. Katsuyama, T. Kurokawa and Y. Osada, Double-network Hydrogels with Extremely High Mechanical Strength, *Adv. Mater.*, 2003, 15(14), 1155–1158.
- J. P. Gong, Materials Both Tough and Soft, *Science*, 2014, 344(6180), 161–162.
- J. P. Gong, Why Are Double Network Hydrogels so Tough?, *Soft Matter*, 2010, 6(12), 2583–2590.
- X. Li, H. Qin, X. Zhang and Z. Guo, Triple-Network Hydrogels with High Strength, Low Friction and Self-Healing by Chemical-Physical Crosslinking, *J. Colloid Interface Sci.*, 2019, 556, 549–556.
- H. Zhang, A. Qadeer, D. Mynarcik and W. Chen, Delivery of Rosiglitazone from an Injectable Triple Interpenetrating Network Hydrogel Composed of Naturally Derived Materials, *Biomaterials*, 2011, 32(3), 890–898.
- S. Shams Es-haghi and R. A. Weiss, Fabrication of Tough Hydrogels from Chemically Cross-Linked Multiple Neutral Networks, *Macromolecules*, 2016, 49(23), 8980–8987.
- X. Wang, F. Zhao, B. Pang, X. Qin and S. Feng, Triple Network Hydrogels (TN Gels) Prepared by a One-Pot, Two-Step Method with High Mechanical Properties, *RSC Adv.*, 2018, 8(13), 6789–6797.
- D. Kaneko, T. Tada, T. Kurokawa, J. P. Gong and Y. Osada, Mechanically Strong Hydrogels with Ultra-low Frictional Coefficients, *Adv. Mater.*, 2005, 17(5), 535–538.
- P. A. Panteli and C. S. Patrickios, Complex Hydrogels Based on Multiply Interpenetrated Polymer Networks: Enhancement of Mechanical Properties via Network Multiplicity and Monomer Concentration, *Macromolecules*, 2018, 51(19), 7533–7545.
- Z. Qiao, Z. Yang, W. Liu, X. Wang, Y. Gao, Z. Yu, C. Zhu, N. Zhao and J. Xu, Molecular Weight Switchable Polyurethanes Enable Melt Processing, *Chem. Eng. J.*, 2020, 384, 123287.
- G. M. Scheutz, J. J. Lessard, M. B. Sims and B. S. Sumerlin, Adaptable Crosslinks in Polymeric Materials: Resolving the Intersection of Thermoplastics and Thermosets, *J. Am. Chem. Soc.*, 2019, 141(41), 16181–16196.
- L. Brunsveld, B. J. B. Folmer, E. W. Meijer and R. P. Sijbesma, Supramolecular Polymers, *Chem. Rev.*, 2001, 101(12), 4071–4098.
- Z. Jiang, A. Bhaskaran, H. M. Aitken, I. C. G. Shackelford and L. A. Connal, Using Synergistic Multiple Dynamic Bonds to Construct Polymers with Engineered Properties, *Macromol. Rapid Commun.*, 2019, 40(10), 1900038.
- H. J. Chen, L. Y. Wang and W. Y. Chiu, *J. Polym. Sci., Part A: Polym. Chem.*, 2008, (112), 551–556.
- M. Röttger, T. Domenech, R. van der Weegen, A. Breuillac, R. Nicolaÿ and L. Leibler, High-Performance Vitrimers from Commodity Thermoplastics through Dioxaborolane Metathesis, *Science*, 2017, 356(6333), 62–65.
- C. Zhang, Z. Yang, N. T. Duong, X. Li, Y. Nishiyama, Q. Wu, R. Zhang and P. Sun, Using Dynamic Bonds to Enhance the Mechanical Performance: From Microscopic Molecular Interactions to Macroscopic Properties, *Macromolecules*, 2019, 52(13), 5014–5025.
- H. Yang, S. Ghiassinejad, E. Van Ruymbeke and C.-A. Fustin, Tunable Interpenetrating Polymer Network Hydrogels Based on Dynamic Covalent Bonds and Metal-Ligand Bonds, *Macromolecules*, 2020, 53(16), 6956–6967.

- 32 B. Zhang, J. Ke, J. R. Vakil, S. C. Cummings, Z. A. Digby, J. L. Sparks, Z. Ye, M. B. Zanjani and D. Konkolewicz, Dual-Dynamic Interpenetrated Networks Tuned through Macromolecular Architecture, *Polym. Chem.*, 2019, **10**(46), 6290–6304.
- 33 L. Zhang, Z. Liu, X. Wu, Q. Guan, S. Chen, L. Sun, Y. Guo, S. Wang, J. Song and E. M. Jeffries, A Highly Efficient Self-healing Elastomer with Unprecedented Mechanical Properties, *Adv. Mater.*, 2019, **31**(23), 1901402.
- 34 P. Song and H. Wang, High-performance Polymeric Materials through Hydrogen-bond Cross-linking, *Adv. Mater.*, 2020, **32**(18), 1901244.
- 35 E. M. Foster, E. E. Lensmeyer, B. Zhang, P. Chakma, J. A. Flum, J. J. Via, J. L. Sparks and D. Konkolewicz, Effect of Polymer Network Architecture, Enhancing Soft Materials Using Orthogonal Dynamic Bonds in an Interpenetrating Network, *ACS Macro Lett.*, 2017, **6**(5), 495–499.
- 36 X. M. Sim, C.-G. Wang, X. Liu and A. Goto, Multistimuli Responsive Reversible Cross-Linking-Decross-Linking of Concentrated Polymer Brushes, *ACS Appl. Mater. Interfaces*, 2020, **12**(25), 28711–28719.
- 37 S. Tajbakhsh, F. Hajiali, K. Guinan and M. Marić, Highly Reprocessable, Room Temperature Self-Healable Bio-Based Materials with Boronic-Ester Dynamic Cross-Linking, *React. Funct. Polym.*, 2021, **158**, 104794.
- 38 J. J. Cash, T. Kubo, D. J. Dobbins and B. S. Sumerlin, Maximizing the Symbiosis of Static and Dynamic Bonds in Self-Healing Boronic Ester Networks, *Polym. Chem.*, 2018, **9**(15), 2011–2020.
- 39 L. Hammer, V. Zee, N. J. and R. Nicolaÿ, Dually Crosslinked Polymer Networks Incorporating Dynamic Covalent Bonds, *Polymers*, 2021, **13**(3), 396.
- 40 N. De Alwis Watuthanthrige, P. Chakma and D. Konkolewicz, Designing Dynamic Materials from Dynamic Bonds to Macromolecular Architecture, *Trends Chem.*, 2021, **3**, 231–247.
- 41 Y. Zeng, W. Yang, S. Liu, X. Shi, A. Xi and F. Zhang, Dynamic Semi IPNs with Duple Dynamic Linkers: Self-Healing, Reprocessing, Welding, and Shape Memory Behaviors, *Polymers*, 2021, **13**(11), 1679.
- 42 B. Zhang, N. De Alwis Watuthanthrige, S. V. Wanasinghe, S. Averick and D. Konkolewicz, Complementary Dynamic Chemistries for Multifunctional Polymeric Materials, *Adv. Funct. Mater.*, 2021, 2108431.
- 43 A. Sharma, S. Kaur, C. G. Mahajan, S. K. Tripathi and G. S. S. Saini, Fourier Transform Infrared Spectral Study of N,N'-Dimethylformamide-Water-Rhodamine 6G Mixture, *Mol. Phys.*, 2007, **105**(1), 117–123, DOI: [10.1080/00268970601146856](https://doi.org/10.1080/00268970601146856).
- 44 S. C. Cummings, O. J. Dodo, A. C. Hull, B. Zhang, C. P. Myers, J. L. Sparks and D. Konkolewicz, Quantity or Quality: Are Self-Healing Polymers and Elastomers Always Tougher with More Hydrogen Bonds?, *ACS Appl. Polym. Mater.*, 2020, **2**(3), 1108–1113.
- 45 J.-Y. Sun, X. Zhao, W. R. K. Illeperuma, O. Chaudhuri, K. H. Oh, D. J. Mooney, J. J. Vlassak and Z. Suo, Highly Stretchable and Tough Hydrogels, *Nature*, 2012, **489**(7414), 133.
- 46 H. Lei, L. Dong, Y. Li, J. Zhang, H. Chen, J. Wu, Y. Zhang, Q. Fan, B. Xue and M. Qin, Stretchable Hydrogels with Low Hysteresis and Anti-Fatigue Fracture Based on Polyprotein Cross-Linkers, *Nat. Commun.*, 2020, **11**(1), 1–10.
- 47 Z. Cao, H. Liu and L. Jiang, Transparent, Mechanically Robust, and Ultrastable Ionogels Enabled by Hydrogen Bonding between Elastomers and Ionic Liquids, *Mater. Horiz.*, 2020, **7**(3), 912–918.